The Multivariable Structure Function and its Application to Helicopter Flight Control Systems Design

J. Liceaga
Departamento de Ingeniería Mecánica
Instituto Tecnológico de Estudios
Superiores de Monterrey CEM
Atizapan, Edo. Mex. C. P. 52926
México

E. Liceaga-Castro
E.L.Castro@gcal.ac.uk
Department of Mathematics
Glasgow Caledonian University
Cowcaddens Road, Glasgow G4 0BA

Abstract

The aim of the paper is to present a novel multivariable control system design framework applied to helicopter flight control. This framework -rather than a method, is based on the definition and the study of the *multivariable structure function* (MSF). The main characteristic of the approach presented here, is that it is application orientated in the sense that it seeks to provide a framework that supports the control design process in the most transparent and direct manner possible, well-suited to the engineering context.

Nomenclature

- A System matrix of the helicopter state space representation
- B Input matrix of the helicopter state space representation
- C Output matrix of the helicopter state space representation
- C_i Input-output channel-i
- $D(s)$ Characteristic polynomial
- e_i Feedback error of channel-i
- F_{ij} $(i-th, jth)$ outloop filter element
- F Outloop filter
- g_{ij} The $(i-th, j-th)$ element or individual transfer function of a transfer matrix
- G Transfer matrix
- k_i Controller associated to channel-i
- m_{ij} $(i-th, jth)$ pre-compensator element
- M Pre-compensator
- r_i Reference signal of channel-i
- p_{ij} $(i-th, jth)$ post-compensator element
- P Post-compensator
- s Laplace operator
- T_z Set of finite transmission zeros
- u_i i-th control input of a system
- X Helicopter state vector
- y_i Output variable associated to channel-i
- Y Output vector
- γ Multivariable structure function of two-input two-output system
- Γ_i Multivariable structure function of channel-i of an m-input m-output system

1 Introduction

Given a multivariable dynamical system, it is possible to define a set of single input-single output transmittances, known as individual channels. In the case of a helicopter these are commonly defined by the pairing of *collective-normal velocity*, *longitudinal cyclic-longitudinal velocity*, *lateral cyclic- lateral velocity* and *collective of tail rotor-heading angle* or *collective of tail rotor-sideslip*. Clearly these pairings arise naturally from the operation of the helicopter. It is shown that using the *multivariable structure function* (MFS) the potential capabilities of every channel in terms of performance, robustness and the degree of interaction with other channels can be evaluated.

From the engineering point of view a set of performance specifications are associated with the definition of the system individual transmittances. For instance, in the case of the helicopter Tischler in Ref. [8] has proposed the following conditions for *Level 1 Handling Qualities*:

1. Every channel should have a bandwidth between $2rad/sec$ and $4rad/sec$,
2. The time response of the channels should be as close as possible to those of typical first order sys-

tems. That is, a phase margin of 90 degrees is requested.

An important feature of the framework proposed is that the use of classical design tools, such as the Bode and Nyquist plots, can be fully exploited in the multivariable context. Moreover, the conditions to which concepts such as gain margins, phase margin and bandwidth can be applied, in the multivariable case, are also elucidated. These facilities permit the helicopter flight control system design to be addressed in terms of customer specifications in a clear, direct and transparent manner.

As the MSF approach is based on the exhaustive analysis of the dynamical structure, it is possible to obtain very simple controllers without sacrificing design specifications. It should be remarked that although the control design is based on individual channels, these are structurally equivalent to the original multivariable system. That is, there is no loss of information.

The paper is composed of the following sections. In Section 1 the control problem of the Lynx at hover is defined.

The definition of the MSF for 2 input-2 output systems and the basic design procedure is included in Section 2. The objective of this section is to review the definition of the MSF which can be represented as a transfer function. It is also shown that the performance capabilities of each individual channel can be determined from the MFS using well known engineering tools (Bode and Nyquist plots). This is followed by a brief account of the generalisation to the m input-m output case.

The dynamic characteristics of the helicopter *Lynx* at hover in the form of its MSF are introduced in Section 3. A solution to the poor properties of the *Lynx* model at hover, due to the highly structured form of the state space representation, is addressed in Section 4. A set of controllers, designed considering the specifications of *Level 1 Handling Qualities* defined in Ref. [8], is presented in Section 5. Decoupling of the channels is achieved by introducing a pre-filter, its design is included in Section 6.

Finally, the conclusions end the paper.

2 Individual channel design: A summary

Individual Channel design (ICD) is an analytical framework in which it is possible to investigate the potential and limitations for feedback design of any multivariable linear time invariant control system.

Although ICD is in principle a feedback structure based on diagonal controllers, it can be applied to any cross coupled multivariable system, irrespective of the degree of coupling. Another important aspect of ICD is that the influence of transmission zeros on the control design and closed loop performance is clearly revealed.

ICD is based on the definition of individual transmision channels. In general the input-output channels arise from design specifications. In this context the control design is an interactive process involving the required specifications, plant characteristics and the multivariable feedback design process itself. Once the channels are defined, that is, the pairing of every output signal to a reference input is established, it is possible to form, with each channel, a feedback loop with a compensator which must be designed to meet *customer* specifications. In this manner the multivariable control design problem is reduced to the design of a single-input single-output control for every channel.

Let for instance a two-input two output plant be represented by

$$\begin{bmatrix} y_1(s) \\ y_2(s) \end{bmatrix} = \begin{bmatrix} g_{11}(s) & g_{12}(s) \\ g_{21}(s) & g_{22}(s) \end{bmatrix} \begin{bmatrix} u_1(s) \\ u_2(s) \end{bmatrix} \quad (1)$$

where $g_{ij}(s)$ represent scalar transfer functions, $y_i(s)$ represent the outputs and $u_i(s)$ the inputs of the system. With $i = 1, 2$ and $j = 1, 2$.

If a diagonal compensator is considered, that is:

$$\begin{bmatrix} u_1(s) \\ u_2(s) \end{bmatrix} = \begin{bmatrix} k_1(s) & 0 \\ 0 & k_2(s) \end{bmatrix} \begin{bmatrix} e_1(s) \\ e_2(s) \end{bmatrix} \quad (2)$$

with $e_i(s) = r_i(s) - y_i(s)$, where $r_i(s)$ represents the plant references, then the input-output channels are defined as:

$$C_i(s) = k_i(s)g_{ii}(s)(1 - \gamma(s)h_j(s)) \quad (3)$$

where $i = 1, 2$ with $i \neq j$, the complex valued function

$$\gamma(s) = \frac{g_{12}(s)g_{21}(s)}{g_{11}(s)g_{22}(s)} \quad (4)$$

is referred to as the **multivariable structure function**. The functions $h_1(s)$ and $h_2(s)$ are:

$$h_i(s) = \frac{k_i(s)g_{ii}(s)}{1 + k_i(s)g_{ii}(s)} \quad \text{where } i = 1, 2 \quad (5)$$

The interaction or cross coupling between the channels can also be evaluated through a transfer function. For instance, the influence of channel-2 on channel-1 is:

$$d_1(s) = \frac{g_{12}(s)}{g_{22}(s)} h_2(s) r_2(s) \quad (6)$$

Similarly, the influence of channel-1 on channel-2 is:

$$d_2(s) = \frac{g_{21}(s)}{g_{11}(s)} h_1(s) r_1(s) \quad (7)$$

Where $r_i(s)$ represents the reference of channel-i ($i = 1, 2$). A block diagram of the feedback system with the diagonal compensator is shown in figures 1 and 2.

It should be emphasised that in the individual channel representation of the multivariable system there is no loss of information. The multivariable character and cross coupling of the plant is contained in the multivariable structure function and the cross coupling terms.

From (3) the magnitude of $\gamma(s)$ may be interpreted as measurement of coupling between the channels. A system whose multivariable structure function has magnitude much smaller than one for all frequencies has a low degree of cross coupling. That is, the channels may be represented by $C_1(s) = k_1(s)g_{11}(s)$ and $C_2(s) = k_2(s)g_{22}(s)$.

The justification for calling $\gamma(s)$ the multivariable structure function arises from the fact that from this function the dynamical structure of the system can be determined. Indeed, the transmission zeros of the system are the zeros of $(1-\gamma(s))$ and the pole-zero structure of the channels is described in terms of $\gamma(s)$ as indicated in Table 1, provided that no pole-zero cancellation occurs in $\gamma(s)$.

In general the poles of $g_{ij}(s)$ are known and the poles of $h_i(s)$ are determined as a part of the control design. On the other hand, the zeros of the channels must be checked in order to find out if any of the channels are nonminimum phase. The control design and channel performance capabilities are determined by the right hand plane zeros (RHPZ's) of the channels, which according to Table 1 are the zeros of $(1-\gamma h_i(s))$ $(i = 1, 2)$. It is well known that the presence of RHPZ's has adverse effects on the control system performance and sensitivity as indicated in Ref. [1, 2].

Transmittance	Zeros	Poles
Channel-C_1	zeros of $(1-\gamma(s)h_2(s))$	poles of $g_{11}, g_{12}, g_{21}, h_2$
Channel-C_2	zeros of $(1-\gamma(s)h_1(s))$	poles of $g_{22}, g_{12}, g_{21}, h_1$

Table 1. Open loop channels poles and zeros.

The potential restrictions on the performance due to non-minimum phase behaviour can be established from the RHPZ's or purely imaginary zeros of $(1-\gamma(s))$. Note that the RHPZ's of $(1-\gamma(s))$ are the RHP transmission zeros of the multivariable system. Moreover, the system has purely imaginary transmission zeros at frequency $s = s_0$ if $\gamma(s_0) = 1$. Clearly the complex valued function $\gamma(s)$ determines the necessary restrictions on $C_1(s)$ and hence of the controller $k_1(s)$.

However, in a more general case it is $(1-\gamma(s)h_i(s))$ which is required to have no RHPZ's and not $(1-\gamma(s))$.

M-input m-output case.

As in the two-input two-output case an m-input m-output system can be decomposed in two subsystems with multiple channels. That is, the original system can be considered to be composed by an m_1-input m_1-output subsystem $\mathbf{M}_1(s)$ and an m_2-input m_2-output subsystem $\mathbf{M}_2(s)$, with $m_1 + m_2 = m$. Under this partition an m-input m-output system can be written as:

$$\mathbf{G}(s) = \begin{bmatrix} \mathbf{G}_{11}(s) & \mathbf{G}_{12}(s) \\ \mathbf{G}_{21}(s) & \mathbf{G}_{22}(s) \end{bmatrix} \tag{8}$$

with output $\mathbf{Y}(s) = col[\mathbf{Y}_1(s),\ \mathbf{Y}_2(s)]$ where $\mathbf{Y}_1(s) = col[y_1(s),\ \dots\ y_{m_1}(s)]$ and $\mathbf{Y}_2(s) = col[y_{m_1+1}(s),\ \dots\ y_{m_2}(s)]$ The input is $\mathbf{U}(s) = col[\mathbf{u}_1(s),\ \ \mathbf{u}_2(s)]$ where $\mathbf{u}_1(s) = col[u_1(s),\ \dots\ u_{m_1}(s)]$ and $\mathbf{u}_2(s) = col[u_{m_1+1}(s),\ \dots\ u_{m_2}(s)]$. Similarly the controller can be partitioned as:

$$\mathbf{K}(s) = \begin{bmatrix} \mathbf{K}_1(s) & 0 \\ 0 & \mathbf{K}_2(s) \end{bmatrix} \tag{9}$$

where $\mathbf{K}_1(s)$ and $\mathbf{K}_2(s)$ are diagonal matrices of order $m_1 \times m_1$ and $m_2 \times m_2$ respectively.

Under the partition proposed the equivalent direct transmittance of subsystem $\mathbf{M}_1(s)$ is:

$$\mathbf{M}_1(s) = [\mathbf{I} - \mathbf{G}_{12}(s)\mathbf{G}_{22}^{-1}(s)\mathbf{H}_2(s)\mathbf{G}_{21}(s)\mathbf{G}_{11}^{-1}(s)]\,\mathbf{G}_{11}(s)\mathbf{K}_1(s) \tag{10}$$

whith the multiple subsystem transfer function

$$\mathbf{H}_2(s) = \mathbf{G}_{22}(s)\mathbf{K}_2(s)[\mathbf{I} + \mathbf{G}_{22}(s)\mathbf{K}_2(s)]^{-1} \tag{11}$$

and is subject to the cross coupling

$$\mathbf{D}_1(s) = \mathbf{G}_{12}(s)\mathbf{G}_{22}(s)^{-1}\mathbf{H}_2(s) \tag{12}$$

The direct transmittance of subsystem $\mathbf{M}_2(s)$ is represented in a similar manner:

$$\mathbf{M}_2(s) = [\mathbf{I} - \mathbf{G}_{21}(s)\mathbf{G}_{11}^{-1}(s)\mathbf{H}_1(s)\mathbf{G}_{12}(s)\mathbf{G}_{22}^{-1}(s)]\,\mathbf{G}_{22}(s)\mathbf{K}_2(s) \tag{13}$$

where

$$\mathbf{H}_1(s) = \mathbf{G}_{11}(s)\mathbf{K}_1(s)[\mathbf{I} + \mathbf{G}_{11}\mathbf{K}_1(s)]^{-1} \tag{14}$$

and with cross coupling

$$\mathbf{D}_2(s) = \mathbf{G}_{21}(s)\mathbf{G}_{11}(s)^{-1}\mathbf{H}_2(s) \tag{15}$$

The pole-zero structure of the open loop multiple channels is described in Table 2.

Transmittance	Zeros	Poles
Subsystem-M_1	zeros of $[\mathbf{I} - \mathbf{G}_{12}\mathbf{G}_{22}^{-1}\mathbf{H}_2\ \mathbf{G}_{21}\mathbf{G}_{11}^{-1}]$	poles of $G_{11}, G_{12}, G_{21}, H_2$
Subsystem-M_2	zeros of $[\mathbf{I} - \mathbf{G}_{21}\mathbf{G}_{11}^{-1}\mathbf{H}_1\ \mathbf{G}_{12}\mathbf{G}_{22}^{-1}]$	poles of $G_{22}, G_{12}, G_{21}, H_1$

Table 2. Open loop channels poles and zeros.

Provided no pole zero cancellation occurs, the transmission zeros, defined by the zeros of $det(\mathbf{G}(s))$ are the same as the zeros of

$$[\mathbf{I} - \mathbf{G}_{12}(s)\mathbf{G}_{22}^{-1}(s)\mathbf{H}_2(s)\mathbf{G}_{21}(s)\mathbf{G}_{11}^{-1}(s)] \quad \text{or} \tag{16}$$

$$[\mathbf{I} - \mathbf{G}_{21}(s)\mathbf{G}_{11}^{-1}(s)\mathbf{H}_1(s)\mathbf{G}_{12}(s)\mathbf{G}_{22}^{-1}(s)] \tag{17}$$

The transmittances of the multiple-channels $\mathbf{M}_1(s)$ and $\mathbf{M}_2(s)$ are together equivalent to the original transfer function matrix $\mathbf{G}(s)\mathbf{K}(s)$, as it has been proven in Ref. [3]. In this case the fundamental indicators of the potential performance (coupling, robustness, and RHP zeros) are indicated by the MSF's associated to the channels $\mathbf{M}_1(s)$ and $\mathbf{M}_2(s)$. The MSF are defined as in Ref. [3]:

$$\Gamma_i(s) = -\frac{det(\mathbf{G}_i^{1,2,\ldots,(i-1)})}{g_{ii}(s)} det(\mathbf{G}^{12\ldots(i-1)i}) \quad (18)$$

where $\mathbf{G}^{12\ldots(i-1)i}$ is the transfer matrix obtained by eliminating k-th rows and columns from $\mathbf{G}(s)$, with $k = 1, 2, \ldots (i-1), i$. $\mathbf{G}_i^{1,2,\ldots,(i-1)}$ is the transfer matrix obtained from $\mathbf{G}(s)$ by setting the diagonal element $g_{ii}(s) = 0$ and eliminating the j-th row and column, with $j = 1, 2, \ldots (i-1)$. By definition $\Gamma_m(s) = 0$. The argument s has been eliminated from (18) for simplicity.

The above definitions can be used to state the following result, which was originally presented in Ref. [3].

Result 3.1 *Consider an m-input m-output system partitioned into two multivariable channels $\mathbf{M}_1(s)$ and $\mathbf{M}_2(s)$ with m_1-input m_1-output and m_2-input m_2-output respectively. Define*

$$\mathbf{G}^*(s) = [\mathbf{I} - \mathbf{G}_{12}(s)\mathbf{G}_{22}^{-1}(s)\mathbf{G}_{21}(s)\mathbf{G}_{11}^{-1}(s)]\mathbf{G}_{11}(s) \quad (19)$$

The two multivariable channels are weakly coupled and thus the multivariable channel $\mathbf{M}_1(s)$ can be designed on the basis of $\mathbf{G}_{11}(s)$ alone provided that:

(i) the diagonal elements of $\mathbf{G}^*(s)$ do not differ significantly from those of $\mathbf{G}_{11}(s)$

(ii) the multivariable structure functions $\Gamma_i(s)$ of the m_1-input m_1-output subsystem $\mathbf{G}^*(s)$ do not differ significantly from those of $\mathbf{G}_{11}(s)$

(iii) the structure (that is the RHPP's and RHPZ's) of $\mathbf{G}^*(s)$ does not differ significantly from that of $\mathbf{G}_{11}(s)$

It should be noted that if the system is decoupled, so that the multivariable channel $\mathbf{M}_1(s)$ can be designed on the basis of the subsystem $\mathbf{G}_{11}(s)$ alone, does not inply that the multivariable channel $\mathbf{M}_2(s)$ can be designed on the basis of $\mathbf{G}_{22}(s)$ alone. As follows it is shown that a hover flight control system can be designed according to this result.

The following analysis relies on investigating the dynamical structure of the input-output channels, that is, the number of RHPP's and RHPZ's of each channel. It is clear from Table 1 that the channels RHPP's are the RHPP's of individual transfer functions. On the other hand, the channels RHPZ's are the RHPZ's of $(1 - \gamma(s)h_i(s))$. Furthermore, the number of RHPZ's of this function can be determined by applying the Nyquist stability criterion. For instance, the number of RHPZ's of $(1 - \gamma(s)h_i(s))$ is given by: $Z = N + P$. Where P is the number of right hand plane poles of $\gamma(s)h_i(s)$ and N is the number of clockwise encirclements of the Nyquist plot of $\gamma(s)h_i(s)$ to the point $(1, 0)$ of the complex plane. In the following subsections the stability criterion of Nyquist, expressed in this context, is extensively used.

3 A helicopter model at hover

The model of the aircraft considered corresponds to the helicopter *Lynx*. Its linearised dynamics at hover were obtained using the simulation software *Helistab*. The linearised rigid body dynamics, assuming quasi-static rotor flapping, are represented by:

$$\dot{\mathbf{X}} = \mathbf{A}\mathbf{X} + \mathbf{B}\mathbf{u} \quad (20)$$

with $\mathbf{X} = col[u,\ w,\ q,\ \theta,\ v,\ p,\ \phi,\ r]$. Where u, v and w represent the longitudinal, lateral and vertical linear velocities in body axis respectively; p, q and r represent the rates of change of the roll, pitch and heading angles respectively and θ and ϕ represent the pitch and roll (Euler) angles respectively. The control input $\mathbf{u} = col[u_1,\ u_2,\ u_3,\ u_4]$ are the commands related to the collective, longitudinal cyclic, lateral cyclic and the tail rotor collective respectively.

The outputs considered are defined as:

$$\mathbf{Y} = \mathbf{C}\mathbf{X} \quad (21)$$

where $\mathbf{Y} = col[C_{11}u + C_{12}w + C_{15}v,\ \theta,\ v,\ r]$. The constants C_{11}, C_{12} and C_{15} are the elements $(1,1)$, $(1,2)$ and $(1,5)$ of the output matrix (21). That is, the first element of $\mathbf{Y}$ is the height rate.

The control problem defined by the output function (21) was originally proposed in Ref. [5].

The transfer matrix function associated to (20) and (21) is:

$$\mathbf{G}(s) = \mathbf{C}(s\mathbf{I} - \mathbf{A})^{-1}\mathbf{B} \quad (22)$$

In order to simplify the notation of polynomials of n-th order the following convention is introduced: let $p(s) = k\ (s + a_1)\ (s + a_2)\ \ldots\ (s + a_n)$ then $p(s)$ will also be written as

$$(s + a_1)(s + a_2)\ldots(s + a_n) \equiv [k, -a_1, -a_2 \ldots, -a_n] \quad (23)$$

Using this notation the characteristic polynomial of the transfer matrix $\mathbf{G}(s)$ is:

$$\begin{aligned} D(s) = \ & [1,\ -10.8743,\ -2.2226,\ 0.2395 \pm 0.5322i, \\ & -0.1811 \pm 0.6026i,\ -0.3224 \pm 0.0066i] \end{aligned} \quad (24)$$

The set of finite transmission zeros is:

$$T_z = \{-0.0094,\ -0.0063\} \quad (25)$$

The MSF's $\Gamma_i(s)$ with $i = 1,\ 2,\ 3$ ($\Gamma_4 = 0$) associated to $\mathbf{G}(s)$ generate the Nyquist plots in figure

3.1. These Nyquist plots lie mainly on the left hand plane for all frequencies, far away from the point $(1,0)$. Therefore, according to the results presented in Ref. [3] and Ref. [6], the representation $\mathbf{G}(s)$ has a dynamic robust structure. The low gain of $\Gamma_1(s)$ and $\Gamma_3(s)$ at all frequencies indicates that some channels may be un-coupled. This aspect can be further investigated by re-arranging $\mathbf{G}(s)$ in the following form:

$$\mathbf{G}_a(s) = \frac{\begin{bmatrix} g_{33}(s) & g_{32}(s) & g_{31}(s) & g_{34}(s) \\ g_{23}(s) & g_{22}(s) & g_{21}(s) & g_{24}(s) \\ g_{13}(s) & g_{12}(s) & g_{11}(s) & g_{14}(s) \\ g_{43}(s) & g_{42}(s) & g_{41}(s) & g_{44}(s) \end{bmatrix}}{D(s)} \tag{26}$$

The Nyquist plot of $\Gamma_1(s)$, $\Gamma_2(s)$ and $\Gamma_3(s)$ of the re-arranged system (26) are exactly the same as those of figure 3.1, but with $T_2(s)$ and $\Gamma_3(s)$ swapped. From these plots some characteristics of the system can be established. For instance:

- due to the large gain of $\Gamma_3(s)$ channels 2 and 3 are coupled and
- $\Gamma_1(s)$ has low gain, thus channel 1 may be decoupled from all the other channels.

These features can be verified by applying the **Result 3.1**. Using this result it can be verified that there is a *near* right hand plane (RHP) Pole-Zero cancellation in channels 1 and 4 and that there is an exact right hand plane Pole-Zero cancellation in channels 3 and 4. It must be noted that the RHP Pole-Zero *near-cancellation* and cancellations are associated to the RHP poles of the system, that is $0.2395 \pm 0.5322i$. This characteristic may be a consequence of the highly structured form of the state-space representation. However, it would not be advisable to ignore it or simply eliminate it due to its unstable characteristic. A solution to this structure problem is addressed next.

4 Structure improvement

A solution to the structure problem addressed above can be obtained by introducing a pre-compensator. This compenstor is added in order to modify the cancellation or *near* cancellation on the RHP of poles-zeros of individual transfer functions into cancellation or *near* cancellation on the LHP. The effectiveness of such a compensator relies on the fact that if an individual transfer function of $\mathbf{G}(s)$ is stabilised by an scalar feedback $m(s)$, all the other elements will be likewise stabilised Ref. [4].

If the pre-compensator only modifies the system around the frequencies of the RHP poles the resulting closed loop system is referred to as *weak feedback*.

As the only minimum-phase individual transfer function of $\mathbf{G}(s)$ (22) is $g_{22}(s)$ the design of the *weak feedback* pre-compensator is constructed around this element, that is:

$$M(s) = \begin{bmatrix} 0 & 0 & 0 & 0 \\ 0 & g_{22}(s) & 0 & 0 \\ 0 & 0 & 0 & 0 \\ 0 & 0 & 0 & 0 \end{bmatrix} \tag{27}$$

A candidate feedback function $m(s)$ is:

$$m(s) = 0.7125\frac{s(s+0.05)(s+2.2)(s^2+0.365s+0.3924)}{(s+0.31)(s+0.5)(s+0.1)(s+0.14)}$$
$$\frac{(s^2+0.6455s+0.1024)}{(s+1)(s+2.5)(s+8)(s^2+0.24s+0.144)} \tag{28}$$

The resulting closed loop system under *weak feedback* is:

$$\mathbf{G}'(s) = (\mathbf{I}+\mathbf{GM})^{-1}\mathbf{G} \tag{29}$$

Where the individual transfer functions are:

$$g'_{22}(s) = \frac{g_{22}(s)}{(1+m(s)g_{22}(s))} \tag{30}$$

$$g'_{k2}(s) = \frac{g_{k2}(s)}{(1+m(s)g_{22}(s))} \quad \text{where } k=1,3,4 \tag{31}$$

$$g'_{2r}(s) = \frac{g_{2r}(s)}{(1+m(s)g_{22}(s))} \quad \text{where } r=1,3,4 \tag{32}$$

$$g'_{ij}(s) = \frac{g_{ij}(s)}{(1+\gamma_{ij}(s)h_{22}(s))} \quad \text{where } i,j=1,3,4 \tag{33}$$

The uncertainty of the individual transfer functions (33) of $\mathbf{G}'(s)$ is not increased if the the Nyquist plots of $\gamma_{ij}(s)h_{22}(s))$ (with $i,j=1,3,4$) do not pass close to the point $(1,0)$. Otherwise, the uncertainty of the individual transfer functions (33) will have been significantly increased. The plots of figures 4.1 show that the Nyquist plots of $\gamma_{ij}(s)h_{22}(s))$ do not pass near the point $(1,0)$.

Result 3.1 can be applied in order to prove that channel-1 of $\mathbf{G}'(s)$ is decoupled from the other channels. Thus, its controller $k_1(s)$ can be designed on the basis of $g'_{11}(s)$ alone.

On the other hand, channel-4 and the multivariable channel associated to channels 2 and 3 remain coupled. In this case, the coupling is the result of a nonminimum phase zero in the fourth row of $\mathbf{G}'(s)$. This fact is illustrated by the Nyquist plots of $\gamma_{44}(s)h_{22}(s)$ and $\gamma_{41}(s)h_{22}(s)$. These functions encircled twice the point $(1,0)$ clockwise. Therefore, the amended individual transfer functions $g'_{41}(s)$ and $g'_{44}(s)$ remain nonminimum phase with RHP zeros similar to those of the original transfer function $g_{41}(s)$ and $g_{44}(s)$. Such a problem can be solved by stabilising the RHP zeros via a post-compensator. This solution does not impose robustness problems as the multivariable structure functions $\Gamma'_1(s)$, $\Gamma'_2(s)$ and $\Gamma'_3(s)$ ($\Gamma'_4(s)=0$) are far from the point $(1,0)$, as shown in Ref. [7].

An example of a post-compensator is:

$$P(s) = \begin{bmatrix} 1 & 0 & 0 & 0 \\ 0 & 1 & 0 & 0 \\ 0 & 0 & 1 & 0 \\ 0 & 0 & p_{43}(s) & 0 \end{bmatrix} \tag{34}$$

where

$$p_{43}(s) = \frac{1.4s}{s^2 + 1.65s + 0.64} \tag{35}$$

The modified system resulted by including the post-compensator is:

$$\mathbf{G}''(s) = \mathbf{P}(s)\mathbf{G}'(s) = \mathbf{P}(s)(\mathbf{I} + \mathbf{GM})^{-1}\mathbf{G} \tag{36}$$

In the pole-zero structure of the modified system (36) only the individual transfer function $g''_{42}(s)$ contains nonminimum phase zeros, which are $0.0828 \pm 0.8468i$.

The dynamic structure of the modified system (36) satisfies the conditions of **Result 3.1**. That is, channel-4 of (36) is decoupled from the other channels, thus its controller $k_4(s)$ can be designed on the basis of $g''_4(s)$. Moreover, channels 2 and 3 of the modified system (36) do not contain pole-zero cancellations on the RHP. The design of the controllers $k_2(s)$ and $k_3(s)$ can be based on the subsystem $\mathbf{G}''_{23}(s)$ alone:

$$\mathbf{G}''_{23}(s) = \begin{bmatrix} g''_{22}(s) & g''_{23}(s) \\ g''_{32}(s) & g''_{33}(s) \end{bmatrix} \tag{37}$$

5 Feedback control design

Level 1 *handling qualities specifications at hover* are defined by having the bandwidth of each channel in the range of $2 - 4\ rad/sec$, Ref. ([8]).

The design of the controllers can be guided by the nature of the multivariable structure functions. For instance, all the Nyquist plots of the original system $\mathbf{G}(s)$ have very low gain from $0.8\ rad/sec$ to infinity, thus controllers $k_2(s)$ and $k_3(s)$ can be designed on the basis of $g''_{22}(s)$ and $g''_{33}(s)$ respectively. That is, for design purposes, subsystem $\mathbf{G}''_{23}(s)$ of equation (37) can be considered decoupled.

Controllers $k_1(s)$ and $k_4(s)$, as indicated above, can be designed by considering only the elements $g''_{11}(s)$ and $g''_{44}(s)$ of the subsystem (37) respectively.

It must be stressed that the changes induced by the *weak feedback* pre-compensator and the post-compensator occur at frequencies far from the range of the design specifications $(2 - 4\ rad/sec)$. Namely, these alterations were introduced in order to improve the structure of the system and to avoid robustness problems whilst introducing the minimum possible changes in the original system.

The system matrix functions of system $G''(s)$ of equation (36) are equivalent to the four individual channels:

$$c_1(s) = k_1(s)g_{11}(s)(1 - \gamma_1(s)) \tag{38}$$

$$c_2(s) = k_2(s)g_{22}(s)(1 - \gamma_2(s)) \tag{39}$$

$$c_3(s) = k_3(s)g_{33}(s)(1 - \gamma_3(s)) \tag{40}$$

$$c_4(s) = k_4(s)g_{44}(s)(1 - \gamma_4(s)) \tag{41}$$

Robustness properties are satisfied if the following points are satisfied:

a. $k_i(s)g_{ii}(s)$, with $i = 1, 2, 3, 4$ have satisfactory positive gain and phase margins,

b. The resulting Nyquist plots of $\gamma_1(s)$, $\gamma_2(s)$, $\gamma_3(s)$ and $\gamma_4(s)$ do not pass near the point $(1, 0)$ for all frequencies and

c. The individual open-loop channels must have adequate gain and phase stability margins within the required channels crossover specifications $(2 - 4\ rad/sec)$

An appropriate set of controllers are:

$$k_1(s) = 1.62\frac{(s^2 + 0.6441s + 0.1040)}{s(s + 0.3362)(s + 50)} \tag{42}$$

$$k_2(s) = 0.52\frac{(s^2 + 0.6s + 0.39)(s^2 + 0.2972s + 0.54)}{s(s + 3)(s + 1)(s + 0.2)(s + 0.0067)} \frac{(s + 0.7)(s + 0.5)}{(s^2 + 0.4s + 0.1696)} \tag{43}$$

$$k_3(s) = -0.2\frac{(s + 11)(s + 2.2)(s^2 + 0.48s + 0.34)}{s(s + 0.12)(s + 0.3)(s + 0.4)(s + 0.2)} \frac{(s^2 + 0.4s + 0.4)(s^2 + 0.64s + 0.102)}{(s + 10)(s^2 + 0.4s + 0.225)} \tag{44}$$

$$k_4(s) = -8.06\frac{(s^2 + 0.645s + 0.104)}{s(s + 0.3139)(s + 50)} \tag{45}$$

The resulting bandwidths for the channels c_1, c_2, c_3 and c_4 are $3.0\ rad/sec$, $2.6\ rad/se$, $2.1\ rad/sec$ and $2.3\ rad/sec$ respectively.

6 Cross-coupling reduction

The cross-coupling among the channels caused by the off diagonal elements of the the closed loop system can be reduced by introducing an input pre-filter.

A design example of a pre-filter which reduces the effects of the off diagonal terms is presented next:

$$F(s) = \begin{bmatrix} 1 & F_{12}(s) & F_{13}(s) & 0 \\ 0 & 1 & F_{23}(s) & 0 \\ 0 & F_{32}(s) & 1 & 0 \\ 0 & F_{42}(s) & F_{43}(s) & 1 \end{bmatrix} \tag{46}$$

where

$$F_{12}(s) = \frac{-s(1000s + 1)}{(68000s^2 + 40680s + 402s + 1)} \tag{47}$$

$$F_{13}(s) = \frac{-19s}{(100s + 1)(3.33s + 1)} \tag{48}$$

$$F_{23}(s) = \frac{-0.4s(s^2 + 0.2s + 0.19)}{(s + 0.08)(s^2 + 1.6s + 1.2)(s + 1)} \frac{1}{(s^2 + 0.6s + 0.6)} \tag{49}$$

$$F_{32}(s) = \frac{0.08s^2}{(0.33s + 1)(0.33s + 1)} \tag{50}$$

$$F_{42}(s) = \frac{0.01s(s + 0.05)}{(s + 0.007)(s + 0.007)(s + 0.1)(s + 0.2)} \frac{(s + 0.06)}{(s + 0.8)(s + 1)} \tag{51}$$

$$F_{43}(s) = \frac{-50s(s + 0.7802s + 7.4524)}{(s + 0.01)(s + 0.2)(s + 1)(s + 1)(s + 2)(s + 2)} \tag{52}$$

The step response shown in figures 6.1 to 6.4 shows that the system has almost been decoupled.

7 Conclusions

The results of the analysis presented show that from the multivariable structure functions it is possible to determine the characteristics of the coupling among the different individual channels, and the number of right hand poles and zeros of every channel.

Further analysis shows that the dynamical structure of the helicopter representation at hover can be improved by eliminating two fictitious non-minimum phase transmssion zeros via *weak feedback*. Further improvements was achieved by including a post-compensator. As a consequence, the helicopter dynamics were reduced - without loss of information- to a two single input-single output systems and a two input-two output system.

Based on the results of the analysis a hover flight control system satisfying *Level 1 Handling Qualities* is presented. The design of the two single input single output control subsystems are obtained according to conventional control methods. While the analysis and design of the multivariable (2 × 2) subsystem is obtained using the multivariable transfer function approach.

Finally, it is shown that by incorporating a reference filter the system (channels) can be decoupled.

A simulation result shows the performance of the design.

References

[1] Freudeuberg J. S. and Loose D. P. *Right half plane poles and zeros and design tradeoffs in feedback systems.* IEEE Transactions in Automatic Control, vol. 30, pp 555-565, 1988.

[2] W. E. Leithead and J. O'Reilly *Uncertain SISO systems with fixed stable minimum-phase controllers: relationship of closed-loop systems to plan RHP poles and zeros.* Int. Journal of Control, 53, pp 771-798, 1991.

[3] W. E. Leithead and J. O'Reilly *m-Input m-output feedback control by individual channel design. Part 1. Struture issues.* Int. J. Control, 1992, vol. 56, No 6, pp 1347-1397.

[4] J. Liceaga-C *Helicopter flight control by individual channel design.* Ph. D. Thesis, Glasgow University, 1994.

[5] M.A. Manness, J.Gribble and D.Murray-Smith. *Multivariable methods for helicopters flight control law design.* Proceedings of the 16th European Rotorcraft Forum, Glasgow. U.K. 1990.

[6] J. O'Reilly and W. E. Leithead, *Multivariable control by individual channel design.* Int. J. Control, 1991, vol. 54, pp 1-46.

[7] E. Leithead and J. O'Reilly. *Performance issues in the individual channel design of 2-input 2-output systems: Part 3. Nondiagonal control and related issues.* Int. J. of Control, N. 55, pp 265-312, 1992.

[8] M. B. Tischler. *Assessment of digital flight control for advanced combat rotorcraft.* J. of the American Helicopter Society, Vol. 34, pp 66-76, 1989.

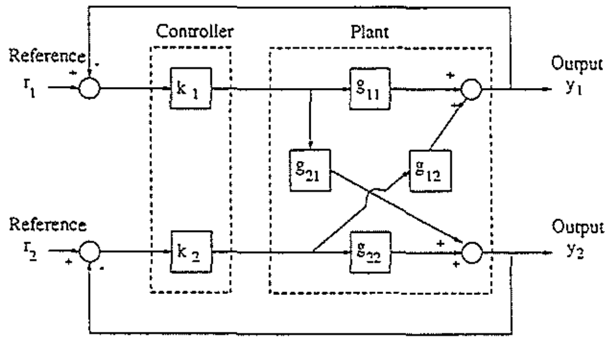

Fig. 2.1 A 2-input 2-output multivariable control with a diagonal controller

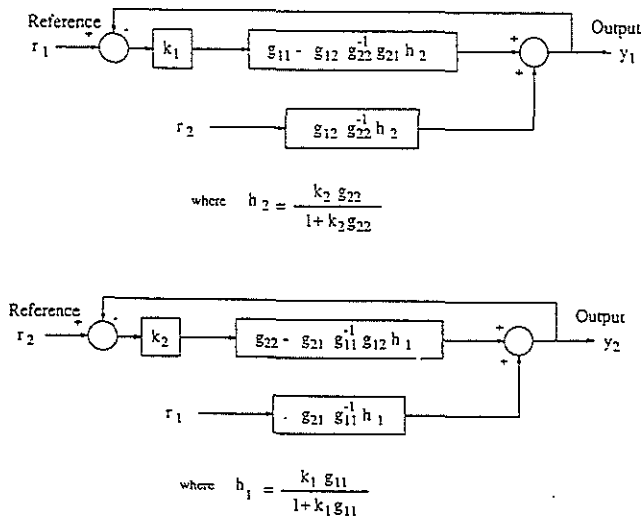

Fig. 2.2 Equivalent input-output channels of a 2-input 2-output multivariable control with a diagonal controller

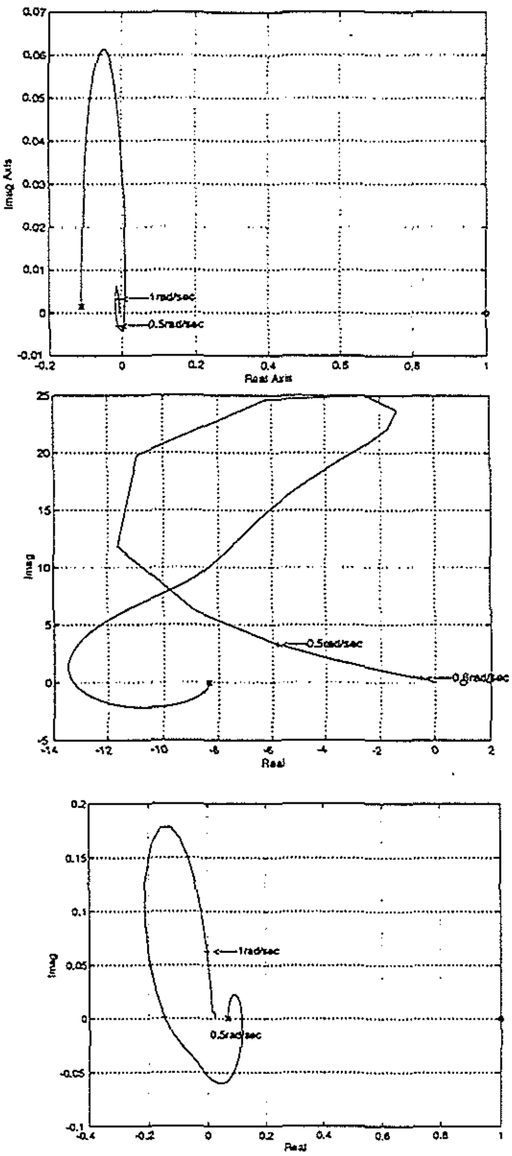

Fig. 3.1 Nyquist plots of $\Gamma_1(s)$, $\Gamma_2(s)$ and $\Gamma_3(s)$ of system $\mathbf{G}(s)$.

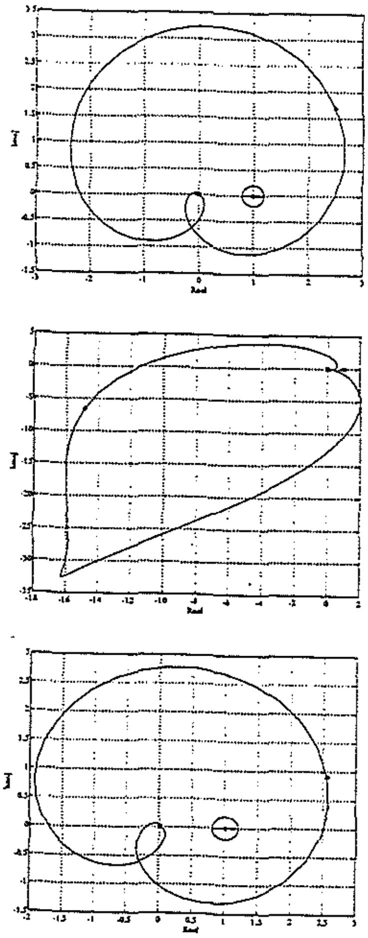

Fig. 4.1 Nyquist plots of $\gamma_{4i}(s)$.

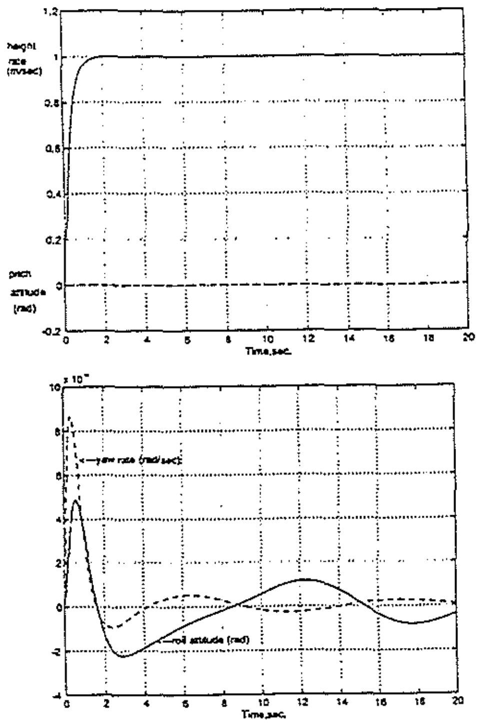

Fig. 6.1 Time response of height rate and pitch attitude to a unity step change of input 1.

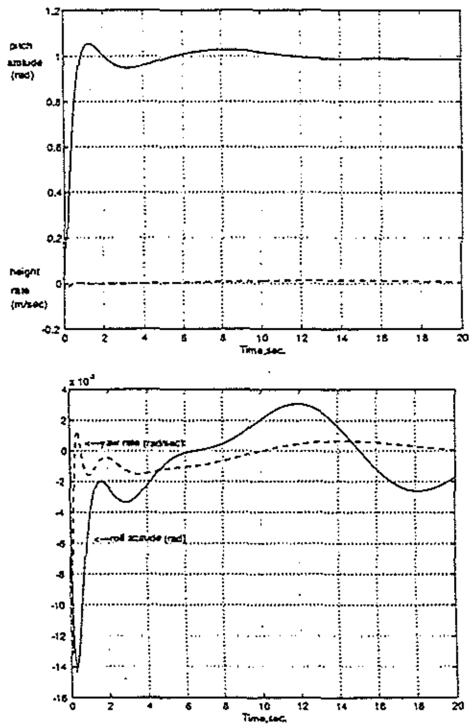

Fig. 6.3 Time response of height rate and pitch attitude to a unity step change of input 2.

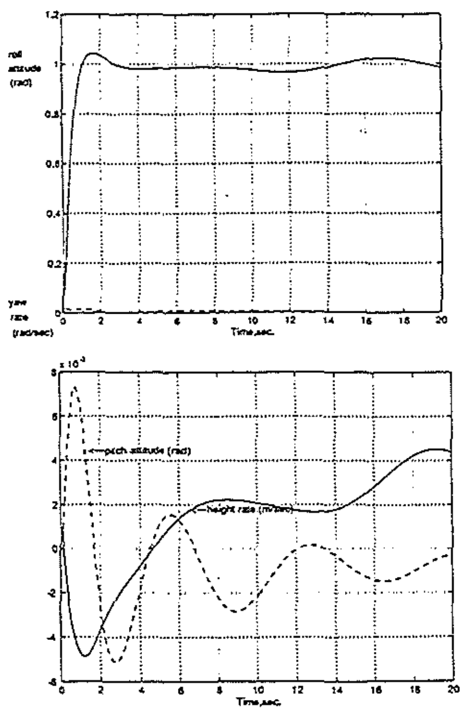

Fig. 6.2 Time response of roll attitude and yaw rate to a unity step change of input 1.

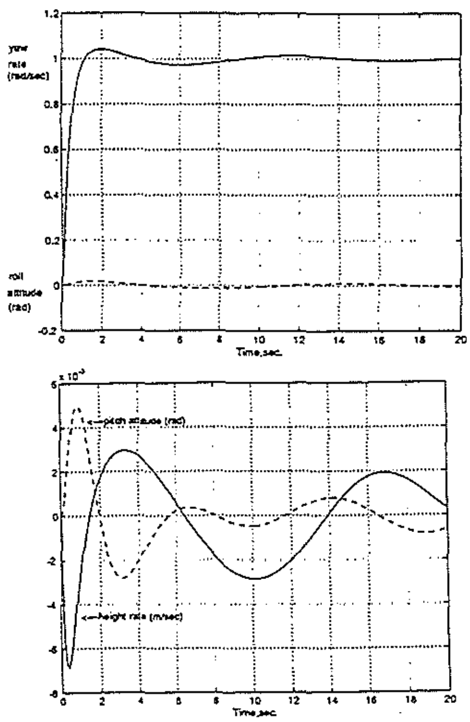

Fig. 6.4 Time response of roll attitude and yaw rate to a unity step change of input 2.